The profile of attentional modulation to visual features

Ming W. H. Fang
Department of Psychology, Michigan State University, East Lansing, MI, USA

Taosheng Liu
Department of Psychology, Michigan State University, East Lansing, MI, USA
Neuroscience Program, Michigan State University, East Lansing, MI, USA

Although it is well established that feature-based attention (FBA) can enhance an attended feature, how it modulates unattended features remains less clear. Previous studies have generally supported either a graded profile as predicted by the feature-similarity gain model or a nonmonotonic profile predicted by the surround suppression model. To reconcile these different views, we systematically measured the attentional profile in three basic feature dimensions—orientation, motion direction, and spatial frequency. In three experiments, we instructed participants to detect a coherent feature signal against noise under attentional or neutral condition. Our results support a nonmonotonic hybrid model of attentional modulation consisting of feature-similarity gain and surround suppression for orientation and motion direction. For spatial frequency, we also found a similar nonmonotonic profile for higher frequencies than the attended frequency, but a lack of attentional modulation for lower frequencies than the attended frequency. The current findings can reconcile the discrepancies in the literature and suggest the hybrid model as a new framework for attentional modulation in feature space. In addition, a computational model incorporating known properties of spatial frequency channels and attentional modulations at the neural level reproduced the asymmetric attentional modulation, thus revealing a connection between surround suppression and the basic neural architecture of an early visual system.

Introduction

Visual attention prioritizes the most important information over other task-irrelevant input from a visual scene. It is well documented that both locations (spatial attention) and features (feature-based attention or FBA) can guide attentional selection (Carrasco, 2011; Liu, 2019). Numerous behavioral and neural studies have demonstrated an enhancement in the representation of the attended location or feature. However, it remains less clear how attentional selection of a location or feature affects the rest of the spatial or feature continuum. Here, we aim to investigate the profile of attentional modulation when selecting visual features within a dimension.

According to the influential feature-similarity gain model, the attended feature is enhanced but such enhancement gradually declines and turns into suppression for unattended features that are progressively more dissimilar to the attended feature. In other words, attentional modulation is a monotonic function of the similarity between attended and unattended feature. Although the feature-similarity gain model was originally proposed in neurophysiological studies to describe attentional modulation of neuronal responses in visual cortex (Martinez-Trujillo & Treue, 2004; Treue & Martinez-Trujillo, 1999), many studies measuring human performance have obtained results consistent with this monotonic profile (Ho, Brown, Abuyo, Ku, & Serences, 2012; Liu, Larsson, & Carrasco, 2007; Saenz, Buracas, & Boynton, 2003; Wang, Miller, & Liu, 2015; Paltoglou & Neri, 2012). However, all these studies have generally employed either two very different test features (e.g., red vs. green, upward vs. downward motion) or a rather coarse sampling of the feature space. Thus, evidence for feature-similarity gain comes from studies testing very dissimilar visual features compared to the attended feature.

When features in close proximity to the attended feature were probed, however, a non-monotonic attentional modulation has been reported (Fang, Becker, & Liu, 2019; Stormer & Alvarez, 2014). Notably, two recent studies on color-based attention have sampled the color space on a fine scale and have found that relative to an attended color, nearby colors were more suppressed than colors further away in the color space (Fang, Becker, & Liu, 2019; Stormer &

Citation: Fang, M. W. H., & Liu, T. (2019). The profile of attentional modulation to visual features. *Journal of Vision*, *19*(13):13, 1–16, https://doi.org/10.1167/19.13.13.

https://doi.org/10.1167/19.13.13 Received July 3, 2019; published November 20, 2019 ISSN 1534-7362

Alvarez, 2014). It is suggested that this "surround suppression" effect enhances signal-to-noise ratio on a fine scale when the target and distractors have similar features. In addition, a further suppression was also observed for very dissimilar colors, thus suggesting both surround suppression and feature-similarity gain are operational but at different similarity scales (Fang, Becker, & Liu, 2019). These results revealed novel attentional modulation profiles in the color domain. However, it is not clear whether these effects are specific to color. Color is a salient visual feature and is known to be particularly effective in guiding attention (e.g., Motter & Belky, 1998; Williams, 1966). Furthermore, color perception is categorical such that continuous changes in the physical input (wavelength) maps onto discrete perceptual categories (e.g., red, blue), which might facilitate a surround suppression effect.

Thus, the profile of attentional modulation for other features remains unclear. Several studies have examined the profile of attentional modulation for orientation and motion direction, with inconclusive evidence for surround suppression (Ho et al., 2012; Tombu & Tsotsos, 2008; Wang et al., 2015). In the orientation domain, Tombu and Tsotsos (2008) found a nonmonotonic attentional modulation such that performance was worst when the cued and target orientations were offset by 45°, followed by a rebound at 90° offset. However, critically, they did not include a baseline condition to establish a genuine suppression effect. For motion direction, Ho and colleagues found a nonmonotonic performance that was lowest at 90° offset between the cued and target direction but fully rebounded at 180°, i.e., opposite direction (Ho et al., 2012). However, this effect is thought to be due to axis-tuned motion mechanisms, which would respond equally well to opposite directions (see also Wang et al., 2015). In other words, the observed rebound effect at 180° could reflect an intrinsic property of motion processing rather than an attentional effect. Lastly, spatial frequency is another feature dimension that is fundamental to early visual processing (De Valois & De Valois, 1988). The profile of attentional modulation to spatial frequency is even less investigated; in particular, whether attention to spatial frequency induces a surround suppression effect is unknown. Taken together, there lacks strong evidence in the literature regarding the modulation profile of FBA in several key feature dimensions.

Therefore, we set out to measure the profile of FBA for three fundamental dimensions in early vision: orientation, motion direction, and spatial frequency. We employed a two-interval forced choice (2-IFC) task, in which participants detected a coherent feature signal. We employed a feature cue to direct FBA (i.e., attention condition) or an uninformative cue to establish baseline performance (i.e., neutral condition). With a fine sampling procedure, we measured performance for targets with different offsets from the cued feature in the attention condition and compared it to the neutral performance to characterize the profile of FBA.

Experiment 1—Orientation

In Experiment 1, we aimed to measure the profile of FBA to orientation. To assess the suppression effect, we included a baseline condition in which no specific orientation was cued. We also used a finer sampling interval (every 15° offset) than previous studies (e.g., Tombu & Tsotsos, 2008) to obtain a more comprehensive mapping of the attentional profile.

Methods

Participants

All participants ($N = 12$, undergraduate students at Michigan State University) had normal or corrected-to-normal visual acuity and gave informed consent. Experimental protocols were approved by the Institutional Review Board at Michigan State University and were performed in accordance with approved guidelines and regulations. Participants were compensated at the rate of $10 per hour.

Apparatus

The stimuli were generated using MATLAB (MathWorks, Natick, MA) and MGL (http://gru.stanford.edu/mgl) and presented on a 21-in. CRT monitor (1,024 × 768 pixels; 120 Hz refresh rate; Dell P992, Round Rock, TX) at a viewing distance of 69 cm. A screen cover with a circular aperture (radius = 11.2 dvg) was used to avoid orientation cues from the screen frames. Participants' heads were stabilized by a chin rest.

Stimulus

The orientation stimuli were two static arrays of tilted lines as an analog to the classic random-dot motion kinematogram (Newsome & Pare, 1988). The stimuli (70% of maximum screen luminance) were presented on a uniform background (50% of maximum screen luminance). Each stimulus array had a total of 180 oriented lines, which were randomly scattered on nine concentric rings (298 possible positions) within an annular region (inner radius = 1.50°; outer radius = 9.93°) centered on the screen. We used only a subset of

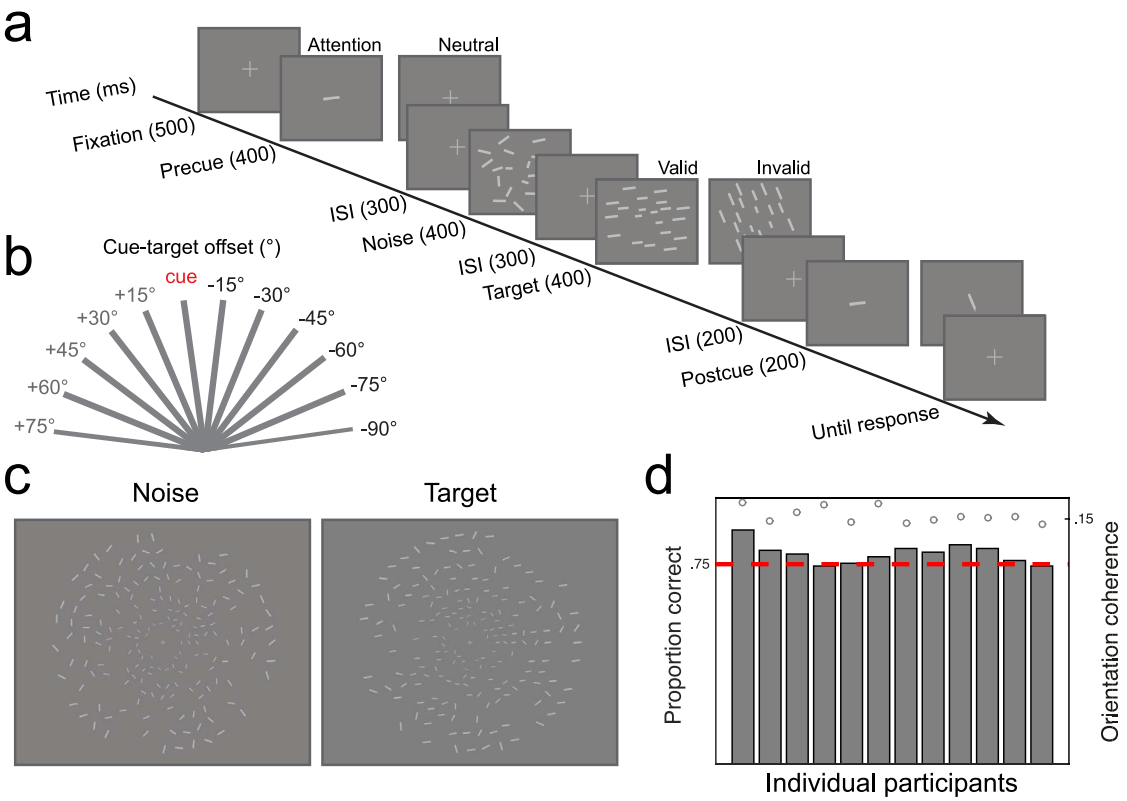

Figure 1. Experiment 1—orientation. (a) Example trial sequence for the 2-IFC task. (b) Depiction of the 12 possible orientations of the coherence signal. The relative offset is shown for all test orientations for a particular cued orientation (in red). (c) More realistic depictions of the actual stimuli (noise and target) used in the experiment. The example target stimulus is drawn at a coherence of 80% in a coherent orientation (8° off horizontal). We did not start from 0° in order to avoid cardinal and oblique orientations (d) Individual participant's baseline performance (bars) and average orientation coherence threshold (circles) across all sessions. Red dashed line represents 75% correct, the intended performance level as controlled by the staircase.

all possible positions to avoid forming obvious contours around the concentric rings. In addition, jitters (up to ± 0.12°) were added to avoid perfect alignment of the lines. To account for cortical magnification, we applied M-scaling to the sizes of lines such that the expected cortical sizes of the lines are equated in V1. To compute the scaling factor, we adapted the original formula in Horton and Hoyt (1991) as follows:

$$M = \frac{E + e_2}{E_{min} + e_2},$$

where M is the scaling factor, E is a line's eccentricity, E_{min} is the eccentricity of lines closest to fixation for a particular stimulus, and e_2 is the eccentricity at which a stimulus subtends half the cortical distance as it subtends at the fovea (3.67°; Dougherty, Koch, Brewer, Fischer, Modersitzki, & Wandell, 2003). The lines closest to fixation had the dimension 0.14° × 0.088°.

In the *target array*, a proportion of lines were drawn in the same orientation, which could be one of 12 fixed orientation values (e.g., from 8° to 173° at a step size of 15°; Figure 1b). The rest were assigned random orientations sampled from 0° to 179° excluding the coherent orientation. In the *noise array,* all lines had randomly sampled orientations from 0° to 179°. The proportion of the same-orientation lines is referred to as orientation coherence, and these lines constituted the signal for the detection task.

Task and procedure

Each experimental session (four in total) consisted of two phases. The first phase was an orientation coherence pretest to determine the coherence threshold for the main task. In the second phase, participants performed the main attention task to measure FBA's modulation profile, which consisted of interleaved neutral precue (i.e., baseline) and orientation precue blocks. Details of the tasks are described as follows.

Orientation coherence pretest

At the beginning of each session, we measured orientation coherence thresholds to control the baseline performance level and equate the task

difficulty across participants, using a QUEST staircase targeting 75% accuracy (Watson & Pelli, 1983). As shown in Figure 1a (Neutral), each trial began with the onset of a fixation cross at the center for 500 ms. A precue appeared for 400 ms, followed by a 300 ms interstimulus interval (ISI). The two stimulus arrays were then shown, each for 400 ms, separated by a 300 ms ISI. After another ISI (200 ms), a postcue (300 ms) was shown to indicate the coherent orientation. After the postcue disappeared, participants reported whether the first or second interval contained the target (the array with a coherent orientation) by pressing one of the two keys on the keyboard. After the response, there was an intertrial interval (ITI) of a blank screen for 500 ms. On each trial, the coherent orientation in the target was randomly drawn from the 12 possible orientations, with the coherence value controlled by the staircase.

Participants were informed that the postcue indicated the target orientation. This was done to eliminate decision uncertainty regarding the orientation on which they should make their judgment (Luck et al., 1994; Pestilli, & Carrasco, 2005). Participants were given unlimited time for response. A tone was played after an incorrect response as feedback. We randomly interleaved two independent staircases (72 trials per staircase) to ensure the accuracy of the coherence threshold estimation. Average of the staircases' estimations was taken as the threshold for each participant in that session.

Attention task

We used an orientation cue to manipulate FBA and measured its effect on detecting the orientation coherence signal. Participants performed the same 2-IFC task as in the pretest under either neutral cue blocks or orientation cue blocks. Orientation coherence was individually determined by the pretest (see aforementioned details). The neutral cue blocks were identical to the pretest, where target orientation was randomly selected from the 12 possible orientations (see Figure 1b) on each trial. For orientation cue blocks, an oriented line ($0.3° \times 0.088°$) was presented at the screen center, which was also randomly selected from the 12 test orientations. The target orientation matched the cue on 60.71% of the trials (valid condition) so that the cue was predictive, and in the rest of trials, the target orientation was randomly assigned to be ±15°, ±30°, ±45°, ±60°, ±75°, or 90° offset from the cued orientation (invalid condition, Figure 1b). Note, for each cue-target offset condition (i.e., 0°, ±15°, ±30°, ±45°, ±60°, ±75°, or 90°), the actual target orientation was equally likely to be one of the 12 test orientations. For each participant, we computed the average performance across the 12 test orientations in the neutral cue blocks as our baseline.

In three separate sessions, participants completed 16 neutral cue blocks (18 trials per block) for a total of 288 neutral trials and 16 orientation cue blocks (126 trials per block) for a total of 2016 orientation cued trials. This yielded 1,224 trials for the valid condition and 72 trials per offset (11 in total, i.e., ±15°, ±30°, ±45°, ±60°, ±75°, and 90°) for the invalid conditions.

Analysis: Model fitting and comparison

We computed cueing effect as the difference in accuracy (measured as proportion of correct responses) between the orientation cue condition and neutral cue condition. We conducted two types of analyses to assess the shape of attentional modulation. In the first analysis, we averaged the cueing effects across the positive and negative offsets and used standard t tests to evaluate enhancement (defined as a positive cueing effect) and suppression (defined as a negative cueing effect) relative to the baseline. In the second analysis, we fit both a monotonic model and a nonmonotonic model to the cueing effect using nonlinear regression to further quantify the surround suppression effect. We included data points up to one point outside the suppressive surround as the data range for fitting the models, based on our previous study showing that farther features are modulated by feature-similarity gain instead of surround suppression (i.e., hybrid profile of FBA; Fang, Becker, & Liu, 2019). Model fitting was performed both on individual participant data and group averaged data. The monotonic model was implemented as a Gaussian function, which had three free parameters:

$$y = \frac{A}{w} e^{-\frac{x^2}{2w^2}} + b,$$

where y is the cueing effect; x is the cue-target offset; and w, A, and b are the free parameters controlling the shape of the function. The nonmonotonic model was implemented as a polynomial function.[1]

$$y = ax^4 + bx^2 + c,$$

where y is the cueing effect, x is the cue-target offset, a, b, and c are the three free parameters controlling the function's shape. To quantify the evidence supporting each model, we computed the Bayesian information criterion (BIC; Schwarz, 1978), with the assumption of a normal error distribution:

$$BIC = n \ln\left(\frac{RSS}{n}\right) + k \ln(n),$$

where n is the number of observations, k is the number of free parameters, and RSS is residual sum of squares

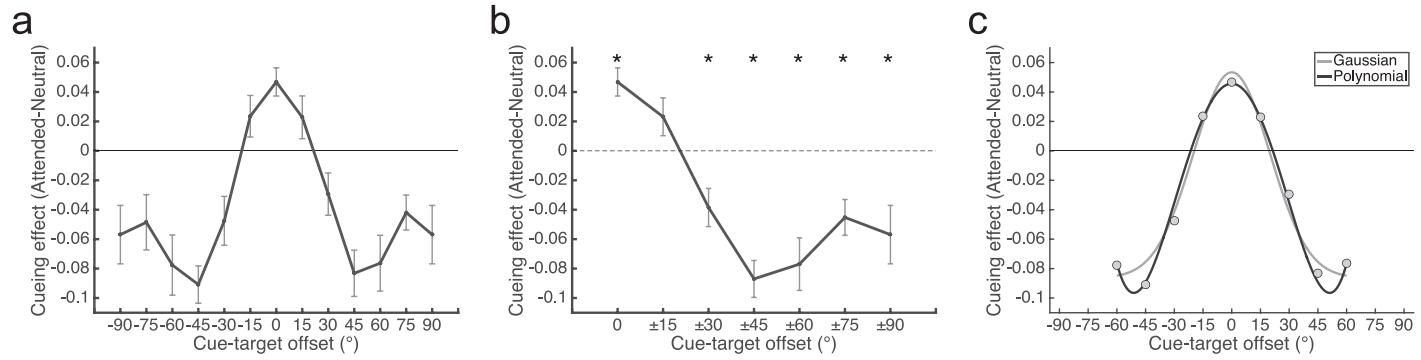

Figure 2. Results for Experiment 1. (a) Average cueing effect for all cue-target offsets. (b) Combined cueing effect. *$p < 0.05$. (c) Model fitting results, showing the fit of both a Gaussian model and a non-monotonic (polynomial) model. Error bar represent standard error of mean.

(Raftery, 1999). We calculated the Bayes factor (*BF*) of the nonmonotonic model over the Gaussian model based on BIC approximation (Wagenmakers, 2007):

$$BF = e^{\left(\frac{(BIC_G - BIC_P)}{2}\right)},$$

where BIC_G is for the Gaussian model, BIC_P is for the polynomial model.

Results

Baseline and cueing effect: Figure 1d depicts participant's baseline performance in the neutral cue condition of the attention test and the corresponding orientation coherence thresholds obtained from the threshold pretest. As expected from our staircase procedure, baselines were well equated across participants in a narrow range around 75% accuracy. Next, we computed the cueing effect for each offset condition by subtracting the baseline performance from the orientation cue condition.

The group-averaged cueing effect is shown in Figure 2a. We found an enhancement when the cue and target were the same (0° offset; valid condition). As the target became more different from the cue, the enhancement decreased and turned into suppression, which reached a maximum around +45°/−45°. Critically, the cueing effect rebounded beyond the maximal suppression up to +75°/−75°, indicating a surround suppression effect. At the largest cue-target offset of 90°, there was a trend of further suppression.

Combined cueing effect: To further characterize the profile of attention, we averaged each participant's cueing effect across the positive and negative offsets because of the symmetric cueing effect (Figure 2b), and then compared against zero in one-sample *t* tests. We corrected *p* values using false discovery rate (FDR; Benjamini & Hochberg, 1995) due to multiple comparisons. Our test showed a significant enhancement at 0° offset (valid condition), $t(11) = 4.89$, $p = 0.0017$, Cohen's $d = 1.41$. At 15° offset, there was no significant cueing effect, $t(11) = 1.8$, $p = 0.099$. As the cue-target offset increased to 30°, we found a significant suppression effect, $t(11) = -2.96$, $p = 0.018$, $d = -0.86$. For further offsets, the suppression effects were all significant: at 45° offset, $t(11) = -6.92$, $p = 0.0002$, $d = -1.99$, at 60° offset, $t(11) = -4.31$, $p = 0.0029$, $d = -1.24$, at 75° offset, $t(11) = -3.71$, $p = 0.006$, $d = -1.071$, and at 90° offset, $t(11) = -2.87$, $p = 0.018$, $d = -0.83$. Critically, this suppression pattern was nonmonotonic. Cueing effect was significantly lower at 45° offset compared to larger offset at 75°, $t(11) = -3.05$, $p = 0.011$, $d = -0.88$, and 0° offset, $t(11) = -9.92$, $p = 1.6 \times 10^{-6}$, $d = -2.86$.

Model comparison: As a complementary analysis, we fitted a monotonic (i.e., Gaussian) model and a nonmonotonic (i.e., polynomial function) model to the average cueing effect. Within the range of −60° to +60° offsets, the nonmonotonic model ($R^2 = 0.99$, $BIC_P = -88.65$) was strongly favored over the monotonic Gaussian model ($R^2 = 0.96$, $BIC_G = -78.77$) with a BF of 139.65, constituting very strong evidence for a surround suppression effect in the attentional modulation (Raftery, 1999). Model comparison based on fitting individual data showed that the non-monotonic model was favored in 10 out of 12 participants.

Discussion

In this experiment, we measured the profile of attention to orientation. Although there is a significant enhancement for valid cue condition, participants' performances were overall worse for invalid conditions, as manifested by significant suppression effects from 30° to 90° offsets. Importantly, the suppression effects showed a non-monotonic profile. The attentional suppression was significantly stronger at 45° offset compared to larger offset at 75°, suggesting a surround suppression effect. In addition, we also observed a significant suppression at the largest offset of 90°,

which is different from a simple rebound effect as predicted by a pure surround suppression. Taken together, the current results revealed both surround suppression and a trend for feature-similarity gain modulation, consistent with a hybrid profile of FBA.

Experiment 2—motion direction

In the second experiment, our goal was to measure the attentional profile for motion direction. Using a similar design as in Experiment 1, we used a 2-IFC task to measure the attentional modulation profile by systematically varying the cue-target directional offset every 15°. We limited our sampling range within −90° to +90° offsets, because a rebound effect beyond ±90° has been observed (Ho et al., 2012; Wang et al., 2015), which could be due to the axis-tuned mechanisms in visual cortex (Albright, 1984; Conway & Livingstone, 2003; Livingstone & Conway, 2003).

Methods

Participants

Another group of participants ($N = 12$; undergraduate students at Michigan State University) gave informed consent. All had normal or corrected-to-normal visual acuity and were compensated at the rate of $10 per hour. Experimental protocols were approved by the Institutional Review Board at Michigan State University. All procedures were performed in accordance with approved guidelines and regulations.

Apparatus and stimulus

The apparatus was the same as in Experiment 1. Stimuli in Experiment 2 were the classic random dot motion kinematograms (Newsome & Pare, 1988), which were composed of moving dots (dot size = 0.1°, speed = 4.5°/s, density = 16.7 dots/deg^2 s^{-1}) presented within an annulus (inner radius = 0.5°, outer radius = 4.5°) centered on the screen on a black background. Three sets of dots were presented in interleaved frames to reduce the possibility of participants tracking individual dots. In the *target array*, a proportion of dots moved in the same direction, which was sampled from 24 fixed motion directions spanning the full direction space every 15° (0° to 345°, as shown in Figure 3b). The remaining dots in the target array had random directions, randomly assigned from 0° to 359° excluding the coherent motion direction. In the *noise array,* all dots moved in random directions (0% coherence). The proportion of the same-direction dots is referred to as motion coherence, and these dots constitute the signal for the detection task.

Task and procedure

We employed the same 2-IFC task and procedure as in Experiment 1 with the following changes. At the beginning of each session, we first measured individual participants' motion coherence thresholds to control baseline task difficulty to be around 75% accuracy level. As depicted in Figure 3a (Neutral), participants performed a 2-IFC task and reported the interval that contained a coherent motion signal under neutral cue condition. On each trial, the coherent target motion direction was assigned randomly to be one of the 24 test directions.

During the attention main test, participants performed the same 2-IFC task under neutral cue blocks, or motion direction cue blocks. The motion direction cue was composed a line (0.4° × 0.088°), which could be in one of the 24 possible test direction. The cue indicated the direction in which the line pointed away from the fixation dot. Participant were trained in practice trials until they fully understood the way target direction was indicated by the cue. In 60% of trials, the target direction matched with the cue (0° offset, valid condition). In the rest of the trials, the target direction could be randomly sampled ±15°, ±30°, ±45°, ±60°, ±75°, or ±90° offset from the cue (invalid conditions, 12 in total). Similar to Experiment 1, for each offset, the actual motion direction was equally likely to be one of the 24 possible test directions. For each participant, we computed the average performance across the 24 test directions in the neutral cue blocks as our baseline.

In four separate sessions, participants completed 16 neutral blocks (18 trials per block) for a total of 288 neutral trials, and 16 direction cue blocks (126 trials per block) for a total of 2,016 trials. This yielded 1,210 trials for the valid condition, and 67 trials per offset (i.e., ±15°, ±30°, ±45°, ±60°, ±75°, and ±90°) for the invalid conditions.

Analysis: Model fitting and comparison

All analyses were the same as in Experiment 1.

Results

Baseline and cueing effect: Figure 3c depicts participant's average baseline performance (i.e., under neutral cue condition) in the main attention test and the average motion coherence thresholds obtained from the threshold pretest. Baselines were within a reasonable range of the desired 75% accuracy level.

Figure 4a shows the average cueing effect of FBA to motion direction. There was an enhancement when the

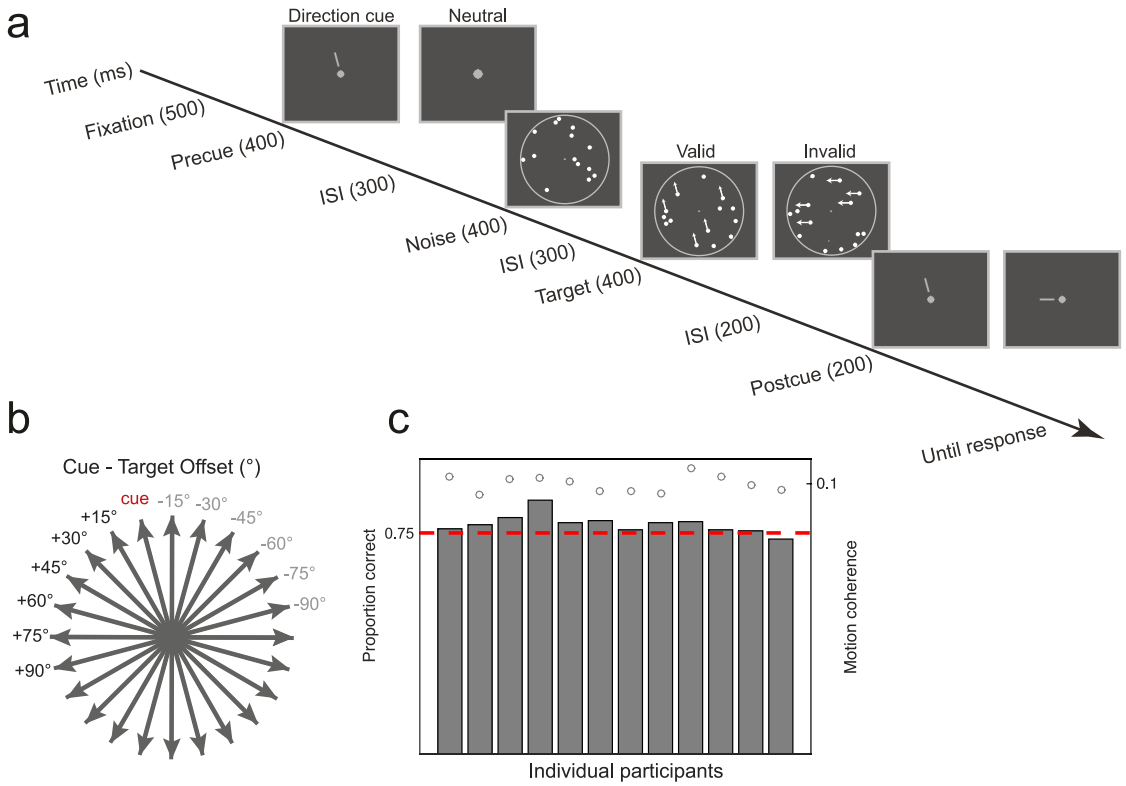

Figure 3. Experiment 2—motion direction. (a) Example trial sequence for the 2-IFC task. (b) Examples for different cue-target offset conditions. Both direction precue and all possible targets direction were uniformly distributed among the 24 possible directions. (c) individual participants' baseline performance (gray bars) and average motion coherence threshold (circles, 75% accuracy level) across all sessions. Red dashed line represents 75% correct, the intended performance level as controlled by the staircase.

cue and target were the same (0° offset; valid condition) as well as a strong suppression effect when the cue and target was most different at +90°/−90° offsets. Importantly, we also found a suppression effect at +45°/−45°offsets followed by a rebound at +60°/−60°, which is consistent with a surround suppression effect.

Combined cueing effect: Following the same procedure in Experiment 1, we averaged the cueing effect across +/− offsets at individual level (Figure 4b), and then conducted one-sample t tests against 0 (FDR corrected). There was a significant enhancement at 0° offset (valid condition), $t(11) = 4.37$, $p = 0.0066$, Cohen's $d = 1.26$ and at 15° offset $t(11) = 3.99$, $p = 0.0066$, $d = 1.15$. There was a significant suppression at 45° offset, $t(11) = -3.82$, $p = 0.0066$, $d = -1.1$, but not at 30° offset, $t(11) = 1.19$, $p = 0.3$; 60° offset, $t(11) = -0.2$, $p = 0.85$; and 75° offset, $t(11) = -1.82$, $p = 0.13$. Such pattern suggested a surround suppression effect elicited by attention to motion direction. Planned comparisons also verified that the nonmonotonic attentional modulation as

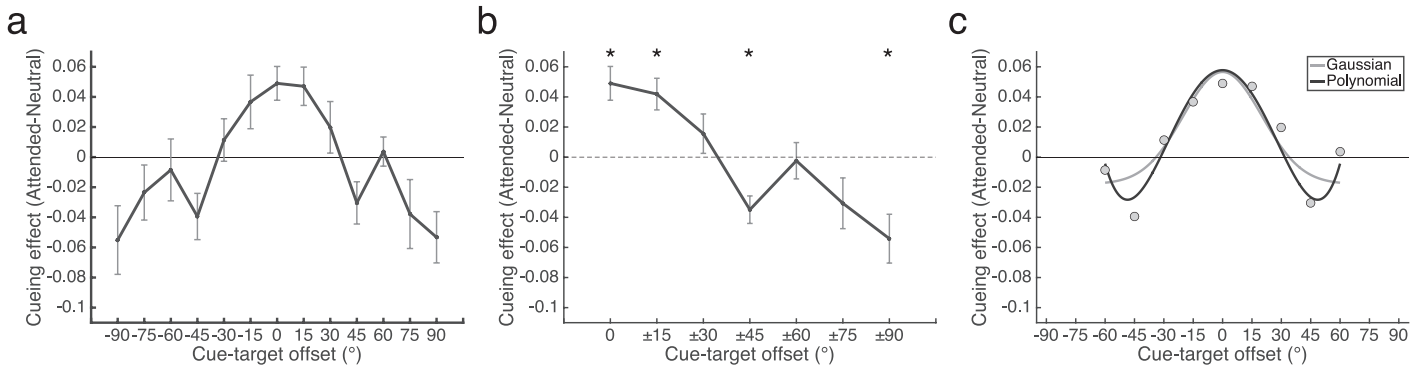

Figure 4. Results for Experiment 2. (a) Group-averaged cueing effect of attention to motion direction, (b) combined cueing effect, *$p < 0.05$. (c) Model fitting results. Error bar represents standard error of mean.

cueing effect at 45° offset was significantly lower compared to the cueing effect at 60° offset, $t(11) = -3.05$, $p = 0.011$, $d = -0.88$, and 0° offset, $t(11) = -9.92$, $p = 1.6 \times 10^{-6}$, $d = -2.86$. Lastly, there was also a further suppression effect when the cue-target was most different at 90°, $t(11) = -3.34$, $p = 0.012$, $d = -0.96$. *Model comparison*: Both a monotonic (i.e., Gaussian) model and a nonmonotonic (i.e., polynomial) model to the average cueing effect (Figure 4c). Following the same procedure in Experiment 1, the largest offset we included were ±60°. The BF (120.8) strongly favored the non-monotonic polynomial model ($R^2 = 0.92$, $BIC_P = -78.96$) over the monotonic Gaussian model ($R^2 = 0.76$, $BIC_G = -69.37$), which constituted very strong evidence for surround suppression effect (Raftery, 1999). For individual participants, we found that the nonmonotonic model was favored in 12 out of 12 participants based on the BIC model evidence.

Discussion

Consistent with Experiment 1, FBA to motion direction also produced a surround suppression at a small scale (e.g., 45° offset) and a feature-similarity gain modulation at a larger scale (e.g., 90° offset). Previous studies have suggested that the rebound in performance beyond 90° offset can be explained by neurons tuned to opposite directions, which lie on a single axis (Ho et al., 2012; Wang et al., 2015). For example, attention to an upward motion may enhance neurons tuned to both upward and downward motion direction. Thus, by limiting our maximum direction offset at 90°, we excluded such axis effect as a possible explanation for our nonmonotonic effect. Thus, the current results provided clear support for a surround suppression modulation at the neighbors of the attended motion direction.

Experiment 3—Spatial frequency

It is well established that a basic function of early visual areas is local spatial frequency analysis (De Valois & De Valois, 1988). However, how attention modulates the processing of spatial frequency information is less clear. In an early study, Rossi and Paradiso showed that attention to the spatial frequency of a central grating modulated the detection of peripheral grating with variable spatial frequencies (Rossi & Paradiso, 1995). However, grating stimuli may not allow an isolation of the attention to spatial frequency as they also contain orientation information. Indeed, Rossi and Paradiso found that attention to spatial frequency also modulated the detection of gratings depending on the task-irrelevant feature — orientation. This finding implied that orientation processing might be obligatory even if participants were instructed to attend to spatial frequency. Thus, it is unclear whether attention to spatial frequencies alone can modulate perception. Moreover, this study found a monotonic attentional profile with a relatively coarse sampling interval of one octave. Thus, the question remains regarding whether a surround suppression could be revealed with a finer sampling.

Methods

Participants

Twelve new participants (undergraduate students at Michigan State University) gave informed consent and participated in this experiment. Experimental protocols were approved by the Institutional Review Board at Michigan State University. All participants had normal or corrected-to-normal visual acuity and were compensated at the rate of $10 per hour.

Apparatus and stimulus

The apparatus was the same as in Experiment 1. There were three types of stimuli: target, noise, and mask. Target stimuli were generated by filtering Gaussian noise images with an isotropic bandpass filter centered on a particular spatial frequency with a bandwidth of 1/10 octaves. Noise stimuli were generated by scrambling the target images. In this experiment, we used visual masks comprised of unfiltered Gaussian noise to avoid ceiling-level performance. Target, noise, and mask stimuli were all windowed by a two-dimensional Gaussian (σ_x, $\sigma_y = 2.67°$) and had the same mean luminance as the background (50% of the maximum luminance).

We chose an intermediate frequency of 1.8 c/° as the cued spatial frequency. Target spatial frequency was sampled from the cued frequency and 8 neighboring frequencies at −2, −1.5, −1, −0.5 octaves (linear scale: 0.45, 0.64, 0.9, 1.27 c/°, respectively), and +0.5, +1, +1.5, +2 octaves (linear scale: 2.55, 3.6, 5.09, 7.2 c/° respectively). The Gaussian noise in the mask contained all possible target frequencies but was uninformative to any specific frequency.

Task and procedure

Contrast threshold pretest

At the beginning of each session, we measured the RMS contrast thresholds for each of the nine test spatial frequencies with a Quest staircase targeting at 75% accuracy level. As illustrated in Figure 5a (Neutral), each trial began with a fixation screen for

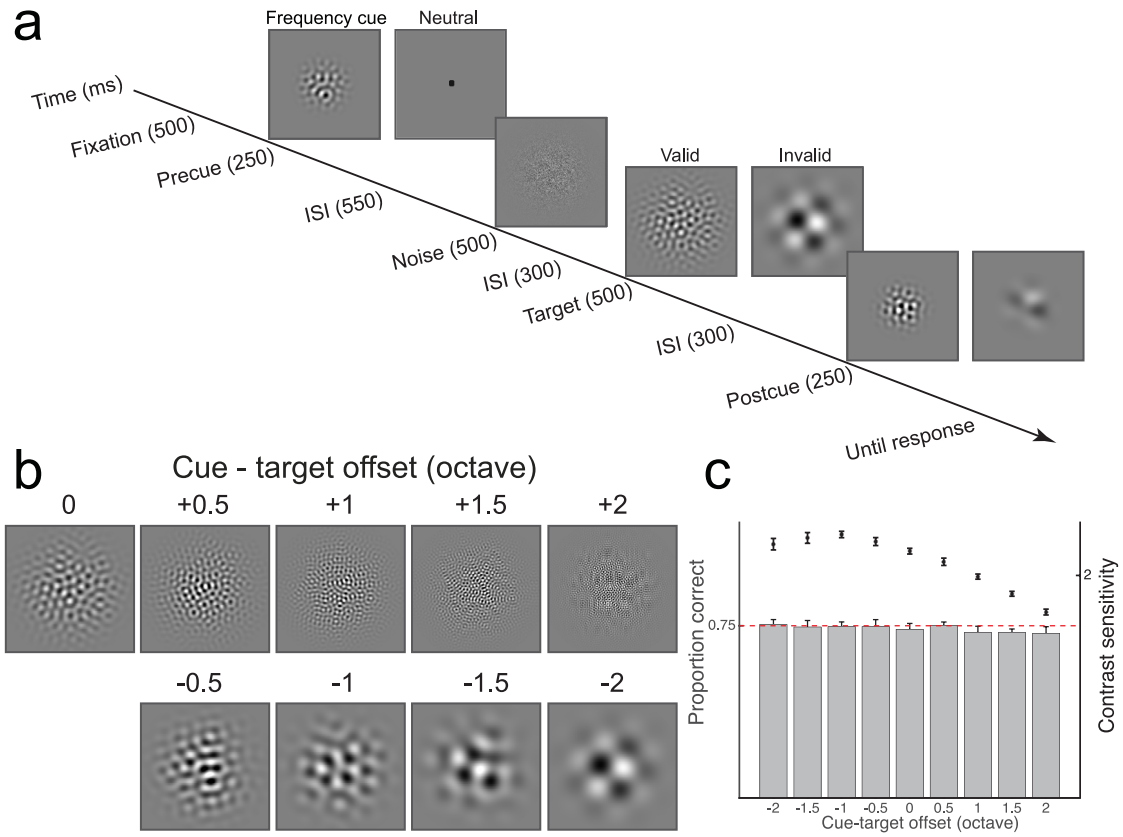

Figure 5. Experiment 3—spatial frequency (SF). (a) Example trial sequence for the 2-IFC task. (b) Examples of target stimulus with different SF offsets from the cued SF. The precue was fixed at 1.8 c/°. (c) Group-averaged baseline performances for all nine targets (in bars). Red dashed line represents 75% correct, the intended performance level as controlled by the staircase. Group-averaged contrast sensitivities were also plotted (in dots), which was calculated as log(1/threshold). Error bars represent standard error of mean. The contrast of the stimuli was increased in this figure for better visualization.

500 ms. A gray fixation dot (0.2°) was then presented for 250 ms. Following a 550 ms ISI, the first stimulus interval appeared for 500 ms. During a stimulus interval, target/noise and visual masks were presented in alternating frames of monitor refresh (frame duration: 8.3 ms, at a refresh rate of 120 Hz). After a 300 ms ISI, the second stimulus interval was present for another 500 ms. After another 300 ms ISI, a postcue (250 ms) was presented to indicate the target spatial frequency. Once the postcue disappeared, participants reported which stimulus interval contained a spatial frequency target by pressing one of two keys on the keyboard. This was followed by a 1,000 ms intertrial-trial interval of a blank screen. Participants were informed that the postcue represented the target spatial frequency, which should help them to make the correct decision. Response time was unlimited. We provided a feedback tone for incorrect responses. Each trial was randomly assigned to one of the nine staircases, to separately measure the contrast threshold for each of the nine spatial frequency targets. The pretest consisted of 12 blocks with 27 trials per block, yielding 36 trials per staircase.

Attention (ain task)

Participants were tested under neutral cue (i.e., fixation dot) blocks or spatial frequency cue blocks with the same 2-IFC task described already. We used the RMS contrast thresholds for each target frequencies as measured during the pretest, which should establish equal baseline performances for different target spatial frequencies under neutral cue condition. For spatial frequency cue blocks, the cue has a fixed spatial frequency of 1.8 c/° , which was windowed by a smaller Gaussian window (σ_x, $\sigma_y = 0.77°$) and always presented at the center of the screen. In 50% of the trials, the target spatial frequency matched with the cue (0 offset; valid condition). Note, the cue was generated at the beginning of each trial such that it was always a different physical image from the target. This is to avoid simple priming effect based on the image pattern. In the other 50% of trials, the target frequencies were randomly selected from eight other test frequencies (±0.5, ±1, ±1.5, and ±2 octaves offset; invalid condition). We used a fixed cue because spatial frequency is a noncircular dimension. Had we used multiple spatial frequency cues, the actual

frequencies in the invalid conditions would differ across different cues and may introduce additional variability in the data.

In three separate sessions, all participants completed 21 neutral blocks (27 trials per block) for a total of 567 neutral trials (63 trials per spatial frequency) and 21 cueing blocks (48 trials per block) for a total of 1,008 cueing trials. This yielded 504 trials for the valid condition and 63 trials per spatial frequency offset for the invalid condition.

Analysis: Model fitting and comparison

All analyses were the same as in Experiment 1, except for the following changes. Due to the asymmetric pattern of attentional modulation (see Results), we fitted both the nonmonotonic and the monotonic model separately to cueing effect for higher and lower target spatial frequencies. Because of the reduced number of data points, for the nonmonotonic model, a second-order polynomial function was used:

$$y = ax^2 + bx + c,$$

where y is the cueing effect, a, b, and c are the three parameters controlling the shape of the function.

Results

Baseline and cueing effect: Figure 5c shows the average contrast sensitivity obtained in the pretest and the average baseline performance measured under neutral cue blocks in the attention task. The average baseline performances for all spatial frequencies were within a narrow range of the target 75% accuracy level.

An asymmetric pattern was found in the cueing effect (Figure 6a). The overall shape showed a robust surround suppression for higher spatial frequency than the cue (i.e., at +1 octave), while the surround suppression for lower spatial frequencies (i.e., at −1 octave) appeared less salient. One-sample t tests against 0 were conducted for each individual offset condition to evaluate attentional enhancement and suppression (FDR corrected). We found a significant enhancement effect when the target spatial frequency matched with the cue, $t(11) = 3.52$, $p = 0.022$, $d = 1.016$. When the target spatial frequency was one octave higher than the cue, there was a significant suppression effect, $t(11) = -3.73$, $p = 0.022$, $d = -1.076$. This suppressive zone was followed by a rebound at +1.5 octaves offset, $t(11) = 0.65$, $p = 0.68$. For negative offsets (i.e., lower spatial frequency than the cue), there was no significant attentional effect (all ps > 0.2).

Model comparison: To further define the shape of the cueing effect, we first fitted both nonmonotonic and monotonic models to the average cueing effect for positive offsets. As shown in Figure 6c, the BF (3,821.6) strongly favored the non-monotonic model ($R^2 = 0.99$, $BIC_P = -40.92$) over the monotonic model ($R^2 = 0.51$, $BIC_G = -24.07$). However, for negative offsets (Figure 6b), the BF (2.14) provided a very weak support for the nonmonotonic model ($R^2 = 0.95$) over the monotonic model ($R^2 = 0.92$). For individual participants, we found that the nonmonotonic model was favored in nine out of 12 participants based on the BIC model evidence for positive offsets. However, for negative offsets, the nonmonotonic model was favored in only four out of 12 participants.

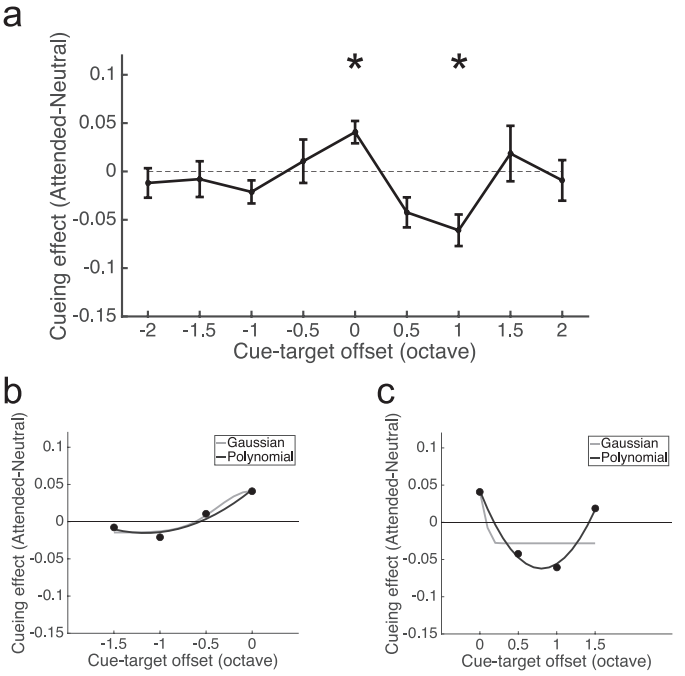

Figure 6. Results for Experiment 3. (a) group-averaged cueing effect. Error bars represent standard error of the mean. *$p <$ 0.05. (b, c) Model fitting for negative offsets (b) and positive offsets (c).

Discussion

We found that FBA to spatial frequency alone can significantly enhance our perceptual processing to the attended spatial frequency as indicated by the enhancement at 0 octave offset. Although this enhancement at 0 offset was similar to orientation and motion, the overall profile of FBA to spatial frequency differed from these other features. First, the suppression was rather weak for the largest offsets (±2 octaves offset), which provide only weak evidence for feature-similarity effect on the coarse scale. Rossi and Paradiso (1995) found that detection of a peripheral grating only showed a strong decrease at 3 octaves offset from the

attended spatial frequency. Hence, it is possible that the ±2 octaves offset may not be sufficiently large to detect suppression due to feature-similarity gain modulation. Second, the profile was asymmetric, such that the nonmonotonic suppression pattern was much more pronounced for higher spatial frequencies than for lower spatial frequencies. We should also note that the sampling interval for lower frequencies was finer than that for the higher frequencies on a linear scale. We will explore the origin of this asymmetric effect in the next section. In sum, we found evidence for surround suppression in FBA to spatial frequencies, although such effect is more robust for spatial frequencies higher than the attended frequency.

General discussion

We measured the profile of FBA to orientation, motion direction, and spatial frequency in three experiments. For orientation and motion, we found a symmetric nonmonotonic modulation, supporting a surround suppression effect in the vicinity of the attended feature. Moreover, the suppression effect reappeared once the cue and target were most different (90° offset, with a stronger effect in motion direction than orientation), which is consistent with a feature-similarity gain modulation. Lastly, we explored the attentional modulation profile for spatial frequency. Our results showed that attention to spatial frequency alone can enhance perceptual sensitivity to the attended frequency. Although the overall shape of the profile was different from orientation and motion, we still found a robust, albeit asymmetric, surround suppression effect as well as a trend for feature-similarity effect. Taken together, our results generally support a hybrid model of both surround suppression and feature-similarity gain that comprises the profile of FBA.

The current study was motivated by previous literature that showed either feature-similarity gain or surround suppression effects, which describe attentional profile *within* a feature dimension. It should be noted that attention can also select whole feature dimensions regardless of feature values (e.g., Found & Muller, 1996; Muller, Heller, & Ziegler, 1995). Interestingly, recent studies (Gledhill, Grimsen, Fahle, & Wegener, 2015; Schledde, Galashan, Przybyla, Kreiter, & Wegener, 2017) found evidence for separate neural effects of dimension- and feature-based attention. Thus, the feature-specific effect (i.e., surround suppression and feature-similarity gain) observed in the current study may be independent from cross-dimensional modulations. However, we did not directly manipulate dimension-based attention in our experiments, and future studies are necessary to assess how such manipulations impact FBA's profiles (i.e., surround suppression and feature-similarity gain).

Profile of FBA to orientation and motion

A previous study also measured attentional modulation profile to orientation and obtained somewhat similar results with our Experiment 1 (Tombu & Tsotsos, 2008). Notably, the lowest performance level was found for orientations at 45° offset to the cued orientation, suggestive of a surround suppression effect. However, our results provided new insights for the profile of FBA. The lack of baseline in this previous study make it impossible to ascertain whether the reduced performance at 45° offset was indeed suppression. Furthermore, participants in this study judged the jaggedness of a grating, which might not require the full use of orientation information (unexpectedly, a nonmonotonic profile was only observed for jagged, but not for straight, stimuli). In our Experiment 1, we introduced a neutral baseline that allowed us to evaluate both enhancement and suppression. In addition, our task required participants to detect a coherent signal defined only in orientation, making orientation the only task-relevant feature. Thus, our results provide stronger evidence for surround suppression in attention to orientation. Our results also demonstrated a trend for feature-similarity gain modulation at the largest cue-target offset that was not observed in the previous study. The overall pattern of our results thus further clarifies that orientation-based attention is consistent with a hybrid profile of both feature-similarity gain and surround suppression effect, instead of a pure surround suppression effect suggested previously.

For motion direction, we also found a hybrid effect of surround suppression and feature-similarity gain modulation. Two previous studies on attention to motion found that task performance monotonically decreased until 90° cue-target offset, then rebounded up to 180° offset (Ho et al., 2012; Wang et al., 2015). Although this overall profile appears to be a surround suppression effect, the full rebound at 180° offset is likely due to an axis effect (Albright, 1984; Conway & Livingstone, 2003; Livingstone & Conway, 2003), rather than a recovery on the far side of suppressive surround. As such, the drop in performance at 90° offset should not be interpreted as a surround suppression effect. By sampling direction offsets at a finer interval (15° interval), we found a suppressive surround at ±45° offset. Our current findings are still compatible with these early studies: If we downsampled our data to every 30° (see Figure 4b), we would have found a cueing effect with a monotonic profile from 0° to 90°, similar to the previous studies (Ho et al., 2012; Wang et al., 2015). Thus, previous studies may

have missed the surround suppression effect because of a relatively coarse sampling in the feature space.

Profile of FBA to spatial frequency

Our results showed that FBA to spatial frequency alone can modulate perception. Although the effects of spatial attention on spatial frequency have been extensively investigated (see Anton-Erxleben & Carrasco, 2013 for a review), much less is known about how FBA modulates the processing of spatial frequency. Rossi and Paradiso (1995) previously showed that attending to the spatial frequency of a center grating modulated the detectability of peripheral gratings with different spatial frequencies in a monotonic fashion. Their results can also be explained by their relative coarse sampling (1 octave) compared to ours (0.5 octave), which could have missed the surround suppression effect. Indeed, when we replotted our data in the same way as their study (see Supplementary Figure S1), we obtained a monotonic profile consistent with their results. Rossi and Paradiso also found that attention to spatial frequency showed feature-selectivity for orientation, indicating an obligatory role of orientation processing with gratings. By using isotropic stimuli, our stimuli provided a better isolation of attention to spatial frequency, without any explicit orientation information. Hence the enhancement and suppression effect in our results reflects perceptual modulation on spatial frequency alone.

Interestingly, we found an asymmetric pattern of attentional modulation in spatial frequency. The attentional surround suppression only occurred for spatial frequencies higher than the cue but not for lower frequencies. In other words, there seems to be an advantage (less suppression) in processing coarser patterns over finer patterns than the cued pattern. This finding is reminiscent of early proposals that perceptual processing of spatial patterns may follow a coarse-to-fine scheme such that the extraction of visual information progresses from a fast but coarse processing to a slow but detailed processing (e.g., Gish, Shulman, Sheehy, & Leibowitz, 1986; Parker & Dutch, 1987; Watt, 1987). These early studies suggested that there could be an intrinsic preference for low spatial frequency contents during initial stages of visual processing. Thus, it is possible that neurons preferring lower frequencies may have been more activated compared to neurons tuned to higher frequencies when attending to the cued frequency. As a result, coarser patterns may be more likely to survive attentional suppression, giving rise to our observed asymmetric pattern of attentional modulation.

A model for asymmetric surround suppression

Although a general advantage in processing low frequency information provides a functional explanation for our observed asymmetric effect, the underlying mechanisms are still unclear. Here we consider potential neural mechanisms for the observed asymmetric surround suppression effect with a computational model of neural population coding (Deneve, Latham, & Pouget, 1999; Ma, Beck, Latham, & Pouget, 2006; Pouget, Dayan, & Zemel, 2000; Pouget, Dayan, & Zemel, 2003). In a previous study, we were able to produce the standard surround suppression effect with such a model (Fang, Becker, & Liu, 2019), if we assume that attending to a feature causes shifts in neural tuning to the attended feature. However, such an effect is symmetric around the cued feature. Here we extended this model to account for the asymmetric effect observed for spatial frequency.

The basic model architecture under neutral condition is shown in Figure 7a (for model details, see Supplementary File S1), which is informed by neurophysiological studies suggesting that spatial frequency-tuned neurons are evenly distributed on a log scale (De Valois & De Valois, 1988). We note that such an arrangement would produce an increase in neuronal tuning width with the preferred spatial frequency on a linear scale (Figure 7b). Similar to our previous work (Fang, Becker, & Liu, 2019), we assumed FBA modulates neuronal tuning in two ways: feature-similarity gain and tuning preference shift (Figure 7d). The key assumption here is that attentional modulation occurs in the original, linear space. However, because the underlying units are not evenly spaced in the linear space, asymmetric effects can occur.

Briefly, the feature-similarity gain modulation was implemented as linear functions that are symmetric near the attended feature on the linear scale (Figure 7d, top panel). The shift in neuronal tuning toward the attended feature, which is based on neurophysiological findings (David, Hayden, Mazer, & Gallant, 2008; Ibos & Freedman, 2014), had an additional scaling factor, due to different tuning width among units in the linear space. Specifically, we assumed that the shift of neuronal tuning scales with the tuning width, such that a larger amount of tuning shift occurs for more broadly tuned units, which correspond to high spatial frequency units in the linear space. We then simulated individual trials of the 2-IFC task under attended and neutral conditions. After obtaining the population responses for both the simulated target and noise stimuli, the model chose the one containing a stronger frequency signal. Model simulations produced an asymmetric cueing effect qualitatively similar to human psychophysical data (cf. Figures 7g and 6a). These results thus suggest that the intrinsic neural architecture (in this

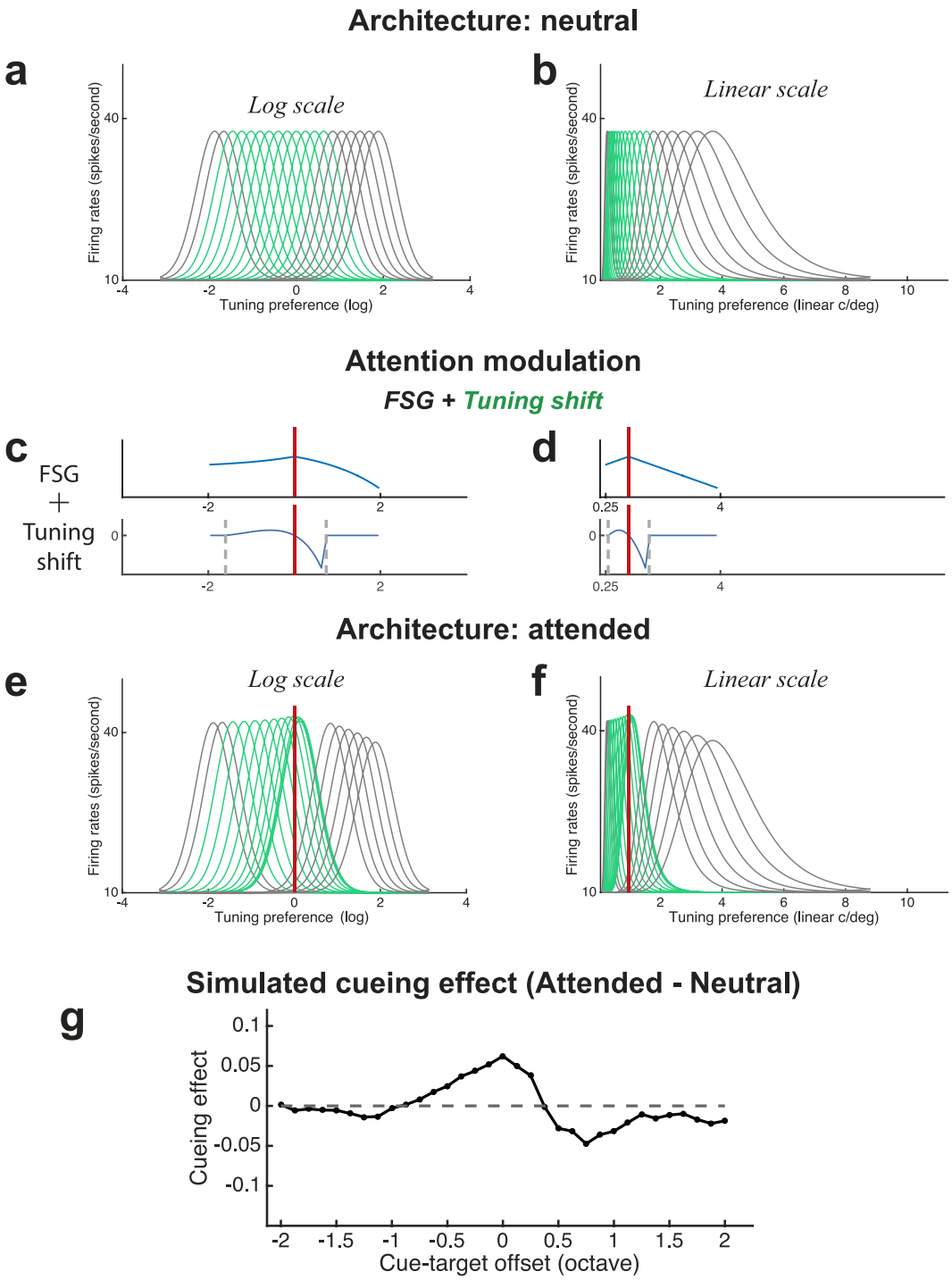

Figure 7. A neural model for the asymmetric surround suppression. (a) Tuning curves in log units (octave) for a subset of the simulated neurons under neutral condition. Green curves represent neurons that are affected by tuning shift. (b) Same tuning curves as in (a) but plotted in linear units (c/°), (c) Feature-similarity gain and tuning shift plotted on log scale (octave), the red solid line labels attended feature. The dashed line labels the range in which neuronal tuning shift occurs. (d) Same as in (c) but plotted on a linear scale (c/°). (e) Tuning curves under a hybrid of feature-similarity gain and tuning shift modulation plotted on log scale (octave). (f) Same as in (e) but plotted on a linear scale (c/°). (g) Simulated cueing effect computed as performance difference between attended and neutral condition. Positive values represent enhancement relative to baseline and negative values represent suppression relative to baseline.

case, unevenly spaced neurons in the linear space) can determine the profile of attentional modulation.

Summary and conclusion

Combined with our previous findings in color-based attention (Fang, Becker, & Liu, 2019), the current study further suggests that surround suppression is a general property of feature-based attention. Previously, we found that color-based surround suppression coincided with color category boundaries. Here, we extend the surround suppression to other non-categorical features, suggesting surround suppression as a canonical effect of FBA. Our study provides a comprehensive characterization of the perceptual consequences of FBA. Although previous studies showed either a surround suppression modulation (e.g., Stormer & Alvarez, 2014; Tombu & Tsotsos, 2008) or a feature-similarity gain modulation (e.g., Ho et al., 2012; Rossi & Paradiso, 1995; Wang et al., 2015), our fine-sampling protocol has revealed a hybrid profile of FBA that unifies the seemingly contradictory modulations in a variety of feature domains. We were also able to reproduce previous findings through resampling our current data on a coarser scale (Ho et al., 2012; Rossi & Paradiso, 1995; Tombu & Tsotsos, 2008; Wang et al., 2015), thus reconciling the apparent discrepancy between previous results and our current results. Lastly, we note that working memory, which is closely related to attention, also has been shown to exhibit surround suppression effect, both in the spatial and feature domain (Fang, Ravizza, & Liu, in press; Kiyonaga & Egner, 2016). Given the suggestion that FBA might be independent from working memory (Mendoza-Halliday & Martinez-Trujillo, 2017; Mendoza, Schneiderman, Kaul, & Martinez-Trujillo, 2011), it would be interesting to investigate whether and how these two cognitive functions may jointly modulate the profile of FBA.

In conclusion, our study demonstrates that feature-similarity gain and surround suppression modulation jointly describe the full profile of FBA. In this way, attention can exert flexible control over perceptual processing such that feature-similarity gain filters out the most distinctive distractors, and surround suppression helps ignore more similar distractors. In addition, while surround suppression is elicited by top-down feature-based attention, where it occurs in the feature space may depend on the basic neural architecture of early visual system, as in the case of spatial frequency.

Keywords: feature-based attention, attentional profile, surround suppression, feature-similarity gain

Acknowledgments

We thank James Cesaro for assistance in data collection. This work was supported by a National Institutes of Health grant (R01EY022727). This work was conceived and designed by M.W.H. Fang and T. Liu. M.W.H. Fang collected and analyzed the data. T. Liu supervised the research. M.W.H. Fang and T. Liu wrote the manuscript. The authors declare no conflicts of interest.

Commercial relationships: none.
Corresponding author: Taosheng Liu.
Email: tsliu@msu.edu.
Address: Michigan State University, Department of Psychology, East Lansing, MI, USA.

Footnote

[1] We have used more canonical Mexican-hat functions, such as the second derivative of Gaussian, in our previous work. Such functions produced similar results for Experiment 1, but they did not provide a good fit for data from the other two experiments. So we used the family of polynomials for all experiments in this report. We used a fourth-order polynomial without the odd-power terms for both Experiments 1 and 2 because of the symmetric shape, and a second-order polynomial for Experiment 3, because we fit the left and right side of the data separately.

References

Albright, T. D. (1984). Direction and orientation selectivity of neurons in visual area MT of the macaque. *Journal of Neurophysiology*, *52*(6), 1106–1130.

Anton-Erxleben, K., & Carrasco, M. (2013). Attentional enhancement of spatial resolution: Linking behavioral and neurophysiological evidence. *Nature Reviews Neuroscience*, *14*(3), 188–200.

Benjamini, Y., & Hochberg, Y. (1995). Controlling the false discovery rate: A practical and powerful approach to multiple testing. *Journal of the Royal Statistical Society. Series B (Methodological)*, *57*, 289–300.

Carrasco, M. (2011). Visual attention: The past 25 years. (2011). *Vision Research, 51*, 1484–1525.

Conway, B. R., & Livingstone, M. S. (2003). Spacetime maps and two-bar interactions of different classes

of direction-selective cells in macaque V1. *Journal of Neurophysiology*, *89*(5), 2726–2742.

David, S. V., Hayden, B. Y., Mazer, J. A., & Gallant, J. L. (2008). Attention to stimulus features shifts spectral tuning of V4 neurons during natural vision. *Neuron*, *59*, 509–521.

Deneve, S., Latham, P. E., & Pouget, A. (1999). Reading population codes: A neural implementation of ideal observers. *Nature Neuroscience*, *2*(8), 740–745.

De Valois, R. L., & De Valois, K. K. (1988). *Spatial vision*. New York: Oxford University Press.

Dougherty, R. F., Koch, V. M., Brewer, A. A., Fischer, B., Modersitzki, J., & Wandell, B. A. (2003). Visual field representations and locations of visual areas V1/2/3 in human visual cortex. *Journal of Vision*, *3*(10), 1–13, https://doi.org/10.1167/3.10.1. [PubMed] [Article]

Fang, M. W. H., Becker, M. W., & Liu, T. (2019). Attention to colors induces surround suppression at category boundaries. *Scientific Reports*, *9*(1), 1443.

Fang, M. W. H., Ravizza, S. M., & Liu, T. (in press). Attention induces surround suppression in visual working memory. *Psychonomic Bulletin & Review*.

Found, A., & Müller, H. J. (1996). Searching for unknown feature targets on more than one dimension: Investigating a "dimension-weighting" account. *Perception & Psychophysics*, *58*(1), 88–101.

Gish, K., Shulman, G. L., Sheehy, J. B., & Leibowitz, H. W. (1986). Reaction times to different spatial frequencies as a function of detectability. *Vision Research*, *26*, 745–747.

Gledhill, D., Grimsen, C., Fahle, M., & Wegener, D. (2015). Human feature-based attention consists of two distinct spatiotemporal processes. *Journal of Vision*, *15*(8):8, 1–17, https://doi.org/10.1167/15.8.8. [PubMed] [Article]

Ho, T. C., Brown, S., Abuyo, N. A., Ku, E.-H. J., & Serences, J. T. (2012). Perceptual consequences of feature-based attentional enhancement and suppression. *Journal of Vision*, *12*(8):15, 1–17, https://doi.org/10.1167/12.8.15. [PubMed] [Article]

Horton, J. C. & Hoyt, W. F. (1991). The representation of the visual field in human striate cortex. A revision of the classic Holmes map. *Archives of Ophthalmology*, *109*(6), 816–824.

Ibos, G., & Freedman, D. J. (2014). Dynamic integration of task-relevant visual features in posterior parietal cortex. *Neuron*, *83*(6), 1468–1480.

Kiyonaga, A., & Egner, T. (2016). Center-surround inhibition in working memory. *Current Biology*, *26*(1), 64–68.

Liu, T. (2019). Feature-based attention: Effects and control. *Current Opinion in Psychology*, *29*, 187–192.

Liu, T., Larsson, J., & Carrasco, M. (2007). Feature-based attention modulates orientation-selective responses in human visual cortex. *Neuron*, *55*, 313–323.

Livingstone, M. S., & Conway, B. R. (2003). Substructure of direction-selective receptive fields in macaque V1. *Journal of Neurophysiology*, *89*(5), 2743–2759.

Luck, S. J., Hillyard, S. A., Mouloua, M., Woldorff, M. G., Clark, V. P., & Hawkins, H. L. (1994). Effects of spatial cuing on luminance detectability: Psychophysical and electrophysiological evidence for early selection. *Journal of Experimental Psychology: Human Perception and Performance*, *20*(4), 887–904.

Ma, W. J., Beck, J. M., Latham, P. E., & Pouget, A. (2006). Bayesian inference with probabilistic population codes. *Nature Neuroscience*, *9*, 1432–1438.

Martinez-Trujillo, J. C., & Treue, S. (2004). Feature-based attention increases the selectivity of population responses in primate visual cortex. *Current Biology*, *14*, 744–751.

Mendoza, D., Schneiderman, M., Kaul, C., & Martinez-Trujillo, J. (2011). Combined effects of feature-based working memory and feature-based attention on the perception of visual motion direction. *Journal of Vision*, *11*(1):11, 1–15, https://doi.org/10.1167/11.1.11. [PubMed] [Article]

Mendoza-Halliday, D., & Martinez-Trujillo, J. C. (2017). Neuronal population coding of perceived and memorized visual features in the lateral prefrontal cortex. *Nature Communications*, *8*(1), 15471.

Motter, B. C., & Belky, E. J. (1998). The guidance of eye movements during active visual search. *Vision Research*, *38*(12), 1805–1815.

Müller, H. J., Heller, D., & Ziegler, J. (1995). Visual search for singleton feature targets within and across feature dimensions. *Perception & Psychophysics*, *57*(1), 1–17.

Newsome, W. T., & Pare, E. B. (1988). A selective impairment of motion perception following lesions of the middle temporal visual area (MT). *Journal of Neuroscience*, *8*, 2201–2211.

Paltoglou, A. E., & Neri, P. (2012). Attentional control of sensory tuning in human visual perception. *Journal of Neurophysiology*, *107*(5), 1260–1274.

Parker, D. M., & Dutch, S. (1987). Perceptual latency and spatial frequency. *Vision Research*, *27*, 1279–1283.

Pestilli, F., & Carrasco, M. (2005). Attention enhances contrast sensitivity at cued and impairs it at uncued locations. *Vision Research*, *45*(14), 1867–1875.

Pouget, A., Dayan, P., & Zemel, R. (2000). Information processing with population codes. *Nature Reviews Neuroscience*, *1*(2), 125–132.

Pouget, A., Dayan, P., & Zemel, R. S. (2003). Inference and computation with population codes. *Annual Reviews Neuroscience*, *26*, 381–410.

Raftery, A. E. Bayes factors and BIC. (1999). *Sociological Methods & Research, 27*, 411–417.

Rossi, A. F., & Paradiso, M. A. (1995). Feature-specific effects of selective visual attention. *Vision Research*, *35*(5), 621–634.

Saenz, M., Buracas, G. T., & Boynton, G. M. (2003). Global feature-based attention for motion and color. *Vision Research*, *43*, 629–637.

Schledde, B., Galashan, F. O., Przybyla, M., Kreiter, A. K., & Wegener, D. (2017). Task-specific, dimension-based attentional shaping of motion processing in monkey area MT. *Journal of Neurophysiology*, *118*(3), 1542–1555.

Schwarz, G. (1978). Estimating the dimension of a model. *The Annals of Statistics*, *6*(2), 461–464.

Stormer, V. S., & Alvarez, G. A. (2014). Feature-based attention elicits surround suppression in feature space. *Current Biology*, *24*(17), 1985–1988.

Tombu, M., & Tsotsos, J. K. (2008). Attending to orientation results in an inhibitory surround in orientation space. *Perception & Psychophysics*, *70*(1), 30–35.

Treue, S., & Martinez-Trujillo, J. C. (1999, June 10). Feature-based attention influences motion processing gain in macaque visual cortex. *Nature*, *399*, 575–579.

Wagenmakers, E. J. (2007). A practical solution to the pervasive problems of p values. *Psychonomic Bulletin & Review*, *14*(5), 779–804.

Wang, Y., Miller, J., & Liu, T. (2015). Suppression effect in feature-based attention. *Journal of Vision*, *15*(5):15, 1–16, https://doi.org/10.1167/15.5.15. [PubMed] [Article]

Watson, A. B., & Pelli, D. G. (1983). QUEST: A Bayesian adaptive psychometric method. *Perception & Psychophysics*, *33*, 113–120.

Watt, R. J. (1987). Scanning from coarse to fine spatial scales in the human visual system after the onset of a stimulus. *Journal of the Optical Society of America A*, *4*, 2006–2021.

Westland, S., & Ripamonti, C. (2004). *Computational colour science using MATLAB*. Chichester: John Wiley & Sons, Ltd.

Williams, L. G. The effect of target specification on objects fixated during visual search. *Perception & Psychophysics*, *1*(5), 315–318 (1966).